A binary star sequence in the outskirts of the disrupting Galactic open cluster UBC 274

Andrés E. Piatti[1,2]★

[1] Instituto Interdisciplinario de Ciencias Básicas (ICB), CONICET UNCUYO, Padre J. Contreras 1300, M5502JMA, Mendoza, Argentina;

[2] Consejo Nacional de Investigaciones Científicas y Técnicas (CONICET), Godoy Cruz 2290, C1425FQB, Buenos Aires, Argentina

ABSTRACT

We report the identification of a numerous binary star population in the recently discovered ∼ 3 Gyr old open cluster UBC 274. It becomes visible once the cluster color-magnitude diagram is corrected by differential reddening and spans mass ratios (q) values from 0.5 up to 1.0. Its stellar density radial profile and cumulative distribution as a function of the distance from the cluster's center reveal that it extends out to the observed boundaries of the cluster's tidal tails (∼ 6 times the cluster's radius) following a spatial distribution indistinguishable from that of cluster Main Sequence (MS) stars. Furthermore, binary stars with q values smaller or larger than 0.75 do not show any spatial distribution difference either. From *Gaia* DR2 astrometric and kinematics data we computed Galactic coordinates and space velocities with respect to the cluster's center and mean cluster space velocity, respectively. We found that, cluster members located all along the tidal tails, irrespective of being a single or binary star, move relatively fast. The projection of their motions on the Galactic plane resembles that of a rotating solid body, while those along the radial direction from the Galactic center and perpendicular to the Galactic plane suggest that the cluster is being disrupted. The similarity of the spatial distributions and kinematic patterns of cluster MS and binary stars reveals that UBC 274 is facing an intense process of disruption that has apparently swept out any signature of internal dynamic evolution like mass segregation driven by two-body relaxation.

Key words. (Galaxy:) open clusters and associations: general – (Galaxy:) open clusters and associations: individual : UBC 274 – technique: photometric.

1. Introduction

UBC 274 (R.A.: $10^h24^m46.50^s$, Dec.: -72°34'28.36", *l*: 292°.3622, b: -12°.7920) is a Galactic open cluster recently discovered by Castro-Ginard et al. (2020) from astrometric, kinematics and photometric data sets available at the *Gaia* DR2 archive[1] (Gaia Collaboration et al. 2016, 2018b,a). They recognized the new object after applying a machine learning based technique and a deep learning artificial neural network. It resulted to be a ∼ 3 Gyr old open cluster (see the cluster color-magnitude diagram (CMD) built by them in Fig, 1) located at ∼ 2 kpc from the Sun. From 365 *bonafide* members, they found that the cluster has a remarkable elongated shape, from which they concluded that it is being the subject of an extensive tidal disruption process.

Because of its populous extra-tidal features, the cluster deserves much more of our attention. For instance, an analysis of the spatial distribution of the different stellar populations in the cluster CMD would contribute to know its ongoing internal dynamical evolutionary stage (see, e.g., Angelo et al. 2019; Piatti et al. 2019a). The relatively deed and complete cluster CMD could also be useful to dive into the still debatable existence of extended Main Sequence (MS) turnoffs in Galactic open clusters and their origin (see, e.g., Cordoni et al. 2018; Piatti & Bonatto 2019; de Juan Ovelar et al. 2020). The position and shape of the observed tidal tails could be used to constrain models of the formation of substructures along them (see, e.g., Montuori et al. 2007; Küpper et al. 2010), among others.

In this work, we closely revisited the *Gaia* DR2 data set for the 365 cluster members identified by Castro-Ginard et al. (2020) and found that UBC 274 contains a well populated binary sequence, that extends out to the observed outskirts of the disrupting cluster following similar spatial and kinematical distributions as escaping single cluster MS stars. If UBC 274 internal dynamics was driven only by two-body relaxation, its binary population should be more centrally concentrated than that of the single stars. As far as we are aware, we report the first open cluster where different spatial distributions of single and binary stars are not observed. The analysis is organized as follows: in Section 2 we present an intrinsic cluster CMD from which we identify the cluster binary star population, while in Section 3 we discuss its resulting spatial and kinematical distributions. Finally, in Section 4 we summarize the main outcomes of this work.

2. The cluster binary star sequence

The presence of differential reddening across the field of star clusters can blur fundamental features of their CMDs. For this reason, we first examined the spatial variation of the interstellar reddening across UBC 274. We built the interstellar reddening map by retrieving the $E(B - V)$ values obtained by Schlafly & Finkbeiner (2011) and provided by NASA/IPAC Infrared Science Archive[2]. Figure 1 depicts the resulting spatial distribution of $E(B - V)$ values, where we superimposed the loci of cluster members, represented by open circles with sizes proportional to
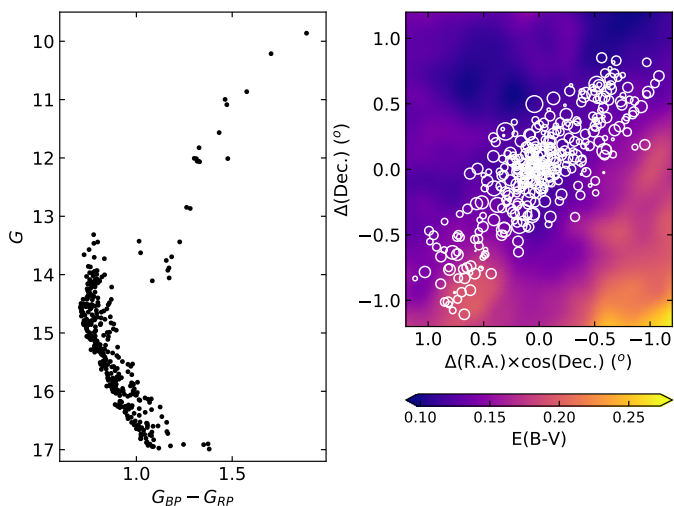
Fig. 1. Observed cluster CMD (left panel). Interstellar reddening ($E(B - V)$) map for the cluster field (right panel). The cluster members are represented by open circles whose sizes are proportional to their G brightnesses.
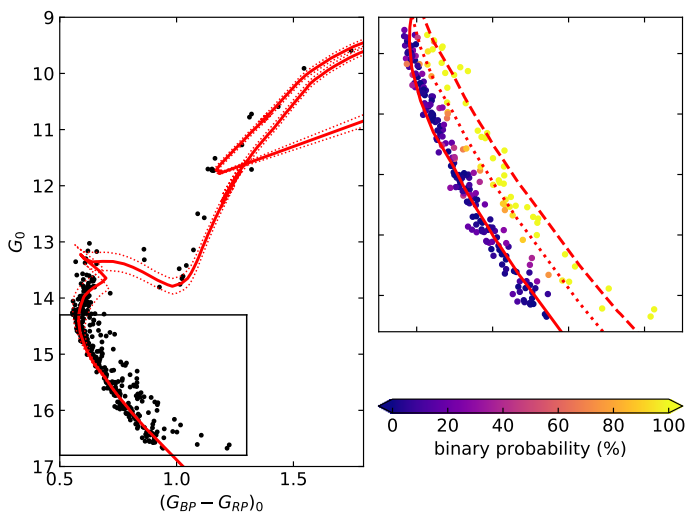
Fig. 2. Intrinsic cluster CMD (left panel). Isochrones of $\log(t /\mathrm{yr}) = 9.45$ (solid line), 9.40 and 9.50 (dotted lines) are superimposed. The rectangle illustrates the zoom-in region depicted in the right panel, where the isochrone of $\log(t /\mathrm{yr}) = 9.45$ is superimposed for $q= 0$, 0.5 and 1.0 with solid, dotted and dashed lines, respectively.

their G brightnesses. As can be seen, the cluster field is affected by some amount of differential reddening. We then corrected by interstellar reddening the G magnitude and $G_{BP} - G_{RP}$ color of each star using the corresponding individual $E(B - V)$ value according to the star's coordinates in the reddening map and the relationships $A_G = 2.44\,E(B-V)$ and $E(G_{BP}-G_{RP})= 1.27\,E(B-V)$ (Cardelli et al. 1989; Wang & Chen 2019). Figure 2 shows the reddened corrected (intrinsic) CMD.

The observed cluster CMD clearly shows a red giant branch, a red clump, a sub-giant branch, a nearly 4 mag long MS and a binary star sequence spanning the whole MS magnitude range. After the reddening correction the binary star sequence is much more pronounced. Hence, we emphasize in the importance of correcting the *Gaia* DR2 photometry by differential reddening as a crucial step to make visible the well delineated and populous cluster binary star strip. Then, we adopted the mean cluster parallax and the cluster metallicity from Castro-Ginard et al. (2020)

and found that the Bressan et al. (2012) theoretical isochrone which best resembles the cluster features, i.e., position and shape of the different giant phases, the MS turnoff and the curvature of the MS, is that of $\log(t /\mathrm{yr}) = 9.45 \pm 0.05$ (2.8±0.2 Gyr) (see Fig. 2, left panel).

We statistically distinguished the cluster binary star population from the cluster MS by running extensive Monte Carlo experiments. We considered the photometric errors in G and $G_{BP} - G_{RP}$ derived by Evans et al. (2018) and the errors in $E(B - V)$ from Schlafly & Finkbeiner (2011), and used the isochrone of $\log(t /\mathrm{yr}) = 9.45$ as a ridge line for the cluster MS from $G_0 = 14.3$ mag down to 16.8 mag (see Fig. 2, right panel). In order to estimate the probability for a star to belong to the cluster MS, we measured the distance from that star to the cluster ridge line, adopting for both end points (the star and the closest position on the cluster ridge line) the corresponding errors in G_0 and $(G_{BP} - G_{RP})_0$. We performed a thousand measurements of such a distance, allowing random values of magnitudes and colors within 3σ for the star and the position on the ridge line, respectively. Then, we considered that a star belongs to the cluster MS if accomplish the criterion: the distance to the MS is less than the sum of the errors along the line connecting the star and the ridge line. We finally obtained the probability (P) of a star to belong to the cluster MS dividing by 10 the number of times it satisfied the above criterion. The difference 100 - P gives the probability of a star to be a binary star. This is because, all the stars are assumed to be cluster member according to the membership criteria applied by Castro-Ginard et al. (2020). Figure 2 (right panel) shows color-coded binary probabilities. In the subsequent analysis we considered binary stars those with $P <$ 40 per cent, which roughly corresponds to secondary to primary mass ratios, $M_2/M_1 = q \gtrsim 0.5$.

3. Analysis and discussion

Using the positions of cluster MS and binary stars we constructed their respective radial density profiles by counting the stars distributed throughout the cluster region (see Fig. 1). Firstly, we split the cluster area in small adjacent boxes of $0°{.}10\times0°{.}10$ that covered the entire analized field. Then, we counted the number of stars (MS and binary stars separately) inside them and computed the mean densities as a function of the distance to the cluster's center (d) by averaging the star counts in every box placed within annulus centered on the cluster with radii d and $d + \Delta d$. This allowed us to estimate the uncertainties in star counts due to stellar fluctuations within each annulus. We repeated this methodology using boxes of increasing size in steps of $0°{.}01$ per side, up to $0°{.}20\times0°{.}20$. The resulting radial density profiles shown in Fig. 3 (left panel) were obtained by averaging all the generated individual density radial profiles. We also built cumulative distributions as a function of d (see Fig. 3, right panel) where the errors were calculated according to the Poisson statistics. For comparison purposes, although suffering from small number statistics, we also constructed the above curves for cluster red giant stars ($G_0 < 13.8$ mag, $(G_{BP} - G_{RP})_0 > 1.0$mag).

Figure 3 reveals that cluster MS and binary stars are distributed following an indistinguishable spatial pattern, from the cluster core region out to the observed boundaries of its tidal tails ($\sim 1°{.}4$ from the cluster' s center). As far as we are aware, binary stars populating cluster tidal tail regions out to ~ 6 times the cluster radius ($\sim 0°{.}22$ for UBC 274) have not been observed in any Galactic open cluster yet. Here we estimated the radius of the cluster main body as the distance r with the highest density contrast, calculated as the ratio between the number of stars inside r
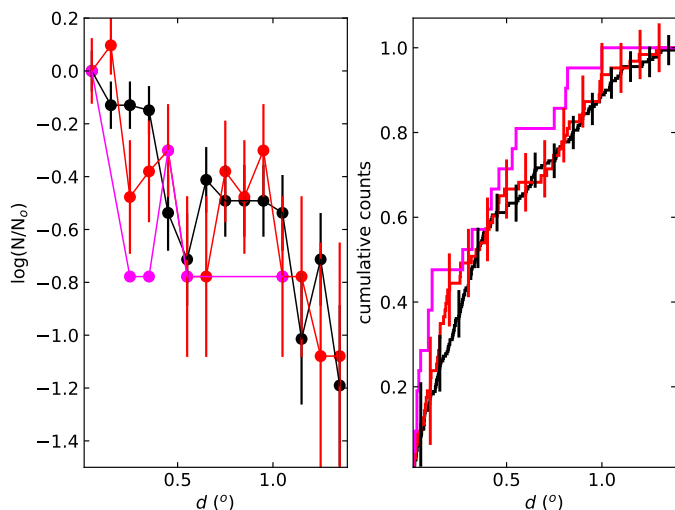
Fig. 3. Observed radial density profiles (left panel) and cumulative distribution functions (right panel) for cluster MS (black lines), binary (red lines), and red giant stars (magenta lines). Error bars are also indicated.

Fig. 4. Associated q values to the cluster binary stars as a function of d, color-coded according to their intrinsic G_0 magnitudes (left panel). The cumulative distribution for binary stars with q values smaller or larger than 0.75 are depicted with a red and black line, respectively (right panel).

to the number of stars in an annulus of interior radius r and equal area. We refer the reader to some detailed studies of open clusters with well known tidal tails, namely: Hyades (Röser et al. 2019), Praesepe (Röser & Schilbach 2019), Coma Berenices (Tang et al. 2019), Blanco 1(Zhang et al. 2020), among others. Furthermore, until now, cluster binary stars have been observed more centrally concentrated than single MS stars, because of mass segregation caused by the dynamics internal evolution driven by two-body relaxation (Reino et al. 2018; Gao 2018; Cohen et al. 2020), even though open clusters have also been subject of tidal effects due to the Milky Way gravitational potential (Piatti & Mackey 2018; Piatti et al. 2019b). We therefore conclude that UBC 274 has become the first open cluster with a numerous binary star population with a unique density profile. The radial and cumulative density profiles of red giant stars, although affected by small number statistics, also hint the removal of the signatures of the internal cluster dynamical evolution.

We further investigated the spatial distribution of the ratio between the mass of the primary (M_1) and that of the secondary (M_2) binary star ($M_2/M_1=q$, $0 \leq q \leq 1$). Following the precepts outlined by Hurley & Tout (1998) and using the theoretical isochrone of log(t /yr)=9.45 (Bressan et al. 2012), we computed the G_0 magnitudes for binary stars with q values from 0.5 up to 1.0 in steps of 0.1 (see Fig. 2, right panel). We then interpolated the CMD positions of the binary stars in the different generated binary star sequences in order to assign them the corresponding q values. Figure 4 (left panel) shows the distribution of q values as a function of d and G_0 magnitudes. As can be seen, more massive binary stars (smaller G_0 magnitudes) are found distributed along the entire d range, irrespective of their q values. This trend is confirmed by the cumulative distribution functions built using binary stars with q values smaller or larger than 0.75 (see Fig 4, right panel). Moreover, both binary star groups also seem to share similar density profiles.

We finally analyzed the kinematics of cluster MS and binary stars from the *Gaia* DR2 coordinates, proper motions, parallaxes and radial velocities. Radial velocities are available for 13 cluster members. For cluster members without RV measurements, we assigned values randomly generated in the range [<RV>−σ(RV),<RV>+σ(RV)], where <RV> and σRV are the cluster mean value and dispersion obtained by Castro-Ginard
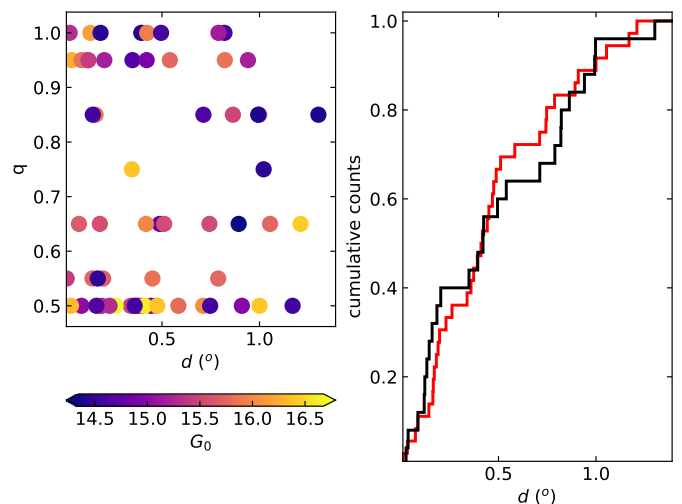
et al. (2020). We computed Galactic coordinates (X, Y, Z) and space velocities (V_X, V_Y, V_Z) employing the astropy[3] package (Astropy Collaboration et al. 2013, 2018), which simply required the input of the astrometric and kinematic data mentioned above. Figure 5 illustrates the space velocity vector field with respect to the mean cluster motion projected on different Galactic planes (coordinates relative to the cluster's center). The figure reveals that both cluster MS and binary stars are moving remarkably fast with respect to the cluster's center all along the tidal tails. In order to better understand that velocity pattern, we plotted in Fig. 6 the spherical components of the space velocities of the stars with respect to the mean cluster velocity as a function of the relative Galactocentric distances of them with respect to the that of the cluster's center. From a kinematical point of view, Fig. 6 provides further support that cluster MS and binary stars located at any position of the cluster main body or tidal tails have similar kinematical behaviors. Additionally it shows that, while projection of the cluster motion on the plane of the Galactic disk rotates like a solid body (bottom panel), the cluster is being disrupted along the direction from the Galactic center (top panel) and along the direction perpendicular to the Galactic plane (middle panel).

4. Conclusions

Motivated by the recent discovery of UBC 274, an ∼ 3 Gyr old open cluster located at ∼ 2 kpc from the Sun, which exhibits extended tidal tails, we revisited the *Gaia* DR2 data set for 365 cluster members.

From the cluster CMD corrected for the differential reddening we recognized a numerous binary star population, distributed along the whole magnitude dynamical range of the cluster MS and toward redder colors. This binary star population spans q values from 0.5 up to 1.0, obtained by interpolation in a set of generated binary star sequences from the theoretical isochrone computed by Bressan et al. (2012) for the cluster's age. We point out that the binary star strip neither is recognized from the ob-

---

[3] https://www.astropy.org
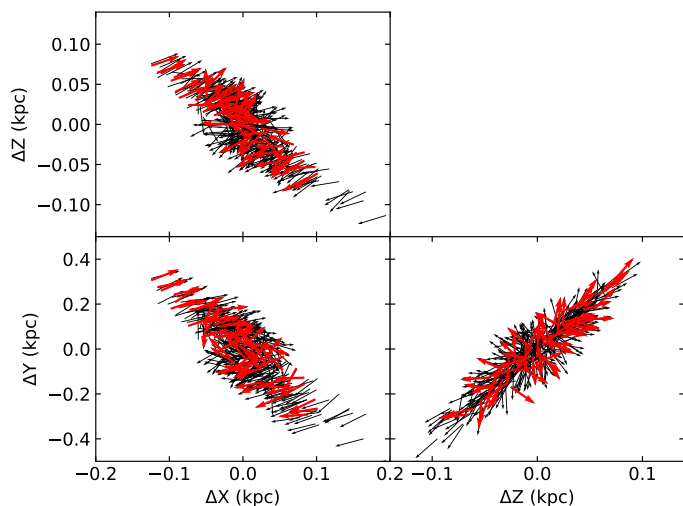
Fig. 5. Space velocity vectors with respect to the mean cluster motion projected on different Galactic planes (relative XYZ coordinates) for cluster MS and binary stars, represented by black and red arrows, respectively.
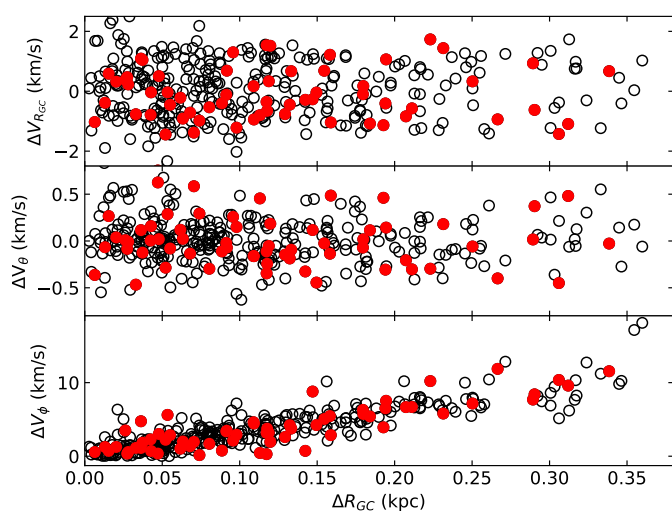
Fig. 6. Difference between individual space velocity components and those of the mean cluster space velocity (spherical coordinate framework) as a function of R_{GC} (relative values).

server cluster CMD nor from that corrected for the the mean cluster reddening.

We built stellar density radial profiles and cumulative distribution functions from the cluster's center out to ~ 6 times its radius for cluster MS and binary stars, separately. The resulting radial profiles and cumulative distributions show that binary stars reach the outermost regions of the observed tidal tails and follow a similar spatial distribution pattern like cluster MS stars. Moreover, in terms of spatial distribution, binary stars with q values smaller or larger than 0.75 do not show any difference either. The outcome that a relatively large number of binary stars populates the cluster tidal tails could become an observational evidence that brings support to the idea that a percentage of the field binary stars comes from disrupted star clusters (Goodwin 2010).

As far as the kinematics of cluster members is considered, we computed Galactic coordinates and space velocity components (cartesian and spherical frameworks) from the astrometric

and kinematic information available. We found that stars located along the cluster's tidal tails, irrespective of being cluster MS or binary stars, are experiencing a relative fast motion with respect to the cluster's center. Particularly, the projected stellar motions on the Galactic plane with respect to the cluster's center resembles that of a rotating solid body, while those along the direction from the Galactic center and perpendicular to the Galactic plane suggest that the clusters is being disrupted. The resulting disrupting directions are in very good agreement with realistic N-body simulations of the orbit of star clusters with tidal tails (e.g., Montuori et al. 2007). The similarity found in the spatial distributions and kinematic patterns of cluster MS and binary stars reveals that UBC 274 is facing an intense process of disruption that has apparently swept out any signature of internal dynamics evolution driven by two-body relaxation.

References

Angelo, M. S., Piatti, A. E., Dias, W. S., & Maia, F. F. S. 2019, MNRAS, 488, 1635
Astropy Collaboration, Price-Whelan, A. M., Sipőcz, B. M., et al. 2018, AJ, 156, 123
Astropy Collaboration, Robitaille, T. P., Tollerud, E. J., et al. 2013, A&A, 558, A33
Bressan, A., Marigo, P., Girardi, L., et al. 2012, MNRAS, 427, 127
Cardelli, J. A., Clayton, G. C., & Mathis, J. S. 1989, ApJ, 345, 245
Castro-Ginard, A., Jordi, C., Luri, X., et al. 2020, A&A, 635, A45
Cohen, R. E., Geller, A. M., & von Hippel, T. 2020, AJ, 159, 11
Cordoni, G., Milone, A. P., Marino, A. F., et al. 2018, ApJ, 869, 139
de Juan Ovelar, M., Gossage, S., Kamann, S., et al. 2020, MNRAS, 491, 2129
Evans, D. W., Riello, M., De Angeli, F., et al. 2018, A&A, 616, A4
Gaia Collaboration, Brown, A. G. A., Vallenari, A., et al. 2018a, A&A, 616, A1
Gaia Collaboration, Helmi, A., van Leeuwen, F., et al. 2018b, A&A, 616, A12
Gaia Collaboration, Prusti, T., de Bruijne, J. H. J., et al. 2016, A&A, 595, A1
Gao, X. 2018, ApJ, 869, 9
Goodwin, S. P. 2010, Philosophical Transactions of the Royal Society of London Series A, 368, 851
Hurley, J. & Tout, C. A. 1998, MNRAS, 300, 977
Küpper, A. H. W., Kroupa, P., Baumgardt, H., & Heggie, D. C. 2010, MNRAS, 401, 105
Montuori, M., Capuzzo-Dolcetta, R., Di Matteo, P., Lepinette, A., & Miocchi, P. 2007, ApJ, 659, 1212
Piatti, A. E., Angelo, M. S., & Dias, W. S. 2019a, MNRAS, 488, 4648
Piatti, A. E. & Bonatto, C. 2019, MNRAS, 490, 2414
Piatti, A. E. & Mackey, A. D. 2018, MNRAS, 478, 2164
Piatti, A. E., Webb, J. J., & Carlberg, R. G. 2019b, MNRAS, 489, 4367
Reino, S., de Bruijne, J., Zari, E., d'Antona, F., & Ventura, P. 2018, MNRAS, 477, 3197
Röser, S. & Schilbach, E. 2019, A&A, 627, A4
Röser, S., Schilbach, E., & Goldman, B. 2019, A&A, 621, L2
Schlafly, E. F. & Finkbeiner, D. P. 2011, ApJ, 737, 103
Tang, S.-Y., Pang, X., Yuan, Z., et al. 2019, ApJ, 877, 12
Wang, S. & Chen, X. 2019, ApJ, 877, 116
Zhang, Y., Tang, S.-Y., Chen, W. P., Pang, X., & Liu, J. Z. 2020, ApJ, 889, 99